The Spine Journal 19 (2019) 762–771

Basic Science

Engineered periosteum-bone biomimetic bone graft enhances posterolateral spine fusion in a rabbit model

Tsai-Sheng Fu, MD*, Ying-Chih Wang, MD, Chien-Hao Chen, MD, Chia-Wei Chang, MD, Tung-Yi Lin, MD, Chak-Bor Wong, MD, Dave Wei-Chih Chen, MD, PhD, Chun-Yi Su, MD

Department of Orthopaedic Surgery, Chang Gung Memorial Hospital, Chang Gung University, No. 222, Maijin Rd, Keelung 20401, Taiwan

Received 23 June 2018; revised 22 September 2018; accepted 24 September 2018

Abstract

BACKGROUND CONTEXT: Bone marrow derived mesenchymal stem cells (BMSCs) and periosteum-derived cells (PDCs) have shown great viability in terms of osteogenic potential and have been considered the major cellular source for skeletal tissue engineering. Using a PDCs-impregnated cell sheet to surround a BMSCs-impregnated tricalcium phosphate (TCP) scaffold might create a periosteum-bone biomimetic bone graft substitute to enhance spine fusion.

PURPOSE: The purpose of this study was to determine the feasibility of using this newly tissue-engineered biomimetic bone graft for posterolateral spine fusion.

STUDY DESIGN/SETTING: This study design was based on an animal model using adult male New Zealand White rabbits.

METHODS: New Zealand White rabbits underwent operation and were divided into three groups based on the experimental material implanted in the bilateral L4–L5 intertransverse space. Group 1 was BMSCs-free TCP wrapped in a PDCs-free cell sheet. Group 2 was BMSCs-loaded-TCP wrapped in a PDCs-free cell sheet. Group 3 was BMSCs-loaded-TCP wrapped in a PDCs-loaded cell sheet. After 12 weeks, six rabbits from each group were euthanized for computed tomography scanning, manual palpation, biomechanical testing, and histology. Each group had 12 radiographic fusion areas for analysis because the right and left intertransverse fusion areas were collected separately.

RESULTS: Radiographic union of 12 fusion areas for groups 1, 2, and 3 was 0, 3, and 9, respectively. Group 3 had significantly higher fusion success than groups 1 and 2 ($p < .001$). Solid fusion of six fusion segments in each group by manual palpation was 0, 1, and 5, accordingly. Group 3 had a higher successful solid fusion rate than groups 1 and 2 (p=.005). The average maximal torques at failure were 727±136 N mm, 627±91 N mm, and 882±195 N mm for groups 1, 2, and 3, accordingly. The maximal torque was significantly higher in group 3 than in group 2 (p=.028). Histological evaluation verified that new bone regeneration were greater in the group 3 samples.

CONCLUSIONS: The results indicated the potential of using a PDCs-impregnated cell sheet to surround the BMSCs-impregnated TCP scaffold for creating a periosteum-bone biomimetic bone graft substitute to enhance bone regeneration and posterolateral fusion success.

Keywords: Artificial cell sheet; Bone marrow mesenchymal stem cells; Bone regeneration; Periosteum-derived cells; Posterolateral fusion; Tissue-engineered bone graft.

FDA device/drug status: Not applicable.

Author disclosures: ***TSF:*** Nothing to disclose. ***YCW:*** Nothing to disclose. ***CHC:*** Nothing to disclose. ***CWC:*** Nothing to disclose. ***TYL:*** Nothing to disclose. ***CBW:*** Nothing to disclose. ***DWCC:*** Nothing to disclose. ***CYS:*** Nothing to disclose.

The disclosure key can be found on the Table of Contents and at www.TheSpineJournalOnline.com.

* Corresponding author. Department of Orthopaedic Surgery, Chang Gung Memorial Hospital, Chang Gung University, No. 222, Maijin Rd, Keelung 20401, Taiwan. Tel.: (866) 2-24313131 ext. 2613; Fax: (886) 2-24332655.

E-mail address: fts111@adm.cgmh.org.tw (Tsai-Sheng Fu, MD.).

https://doi.org/10.1016/j.spinee.2018.09.013

Introduction

Successful surgical management of skeletal defects often requires bone grafting for healing. Autogenous bone graft remains the gold standard for successful skeletal defect repair. However, several concerns, such as limited availability, donor site morbidities, increased blood loss, and increased operative time, have prompted the search for suitable alternatives [1–3].

Tissue engineering strategies have emerged as an alternative and hold great promise for regenerating musculoskeletal tissues. One important component is the three-dimensional (3D) artificial scaffold, which serves as a temporary support structure and imparts the necessary biophysical, biomechanical, and biochemical cues required for cell attachment, proliferation, and differentiation to form tissue [4]. Although the bone marrow derived mesenchymal stem cells (BMSCs) have been considered the major cellular source for skeletal tissue engineering, there are some shortfalls including the low number of cells yielded by isolated adult BMSCs, the cellular senescence, and limited proliferation capacity [5–10].

During the past decade, the periosteum has been reported to have remarkable regenerative capacity. It is a bi-layered membrane composed of a fibrous outer layer, which adheres to a thin inner cambium layer that is adjacent to the bone. The periosteum provides pluripotent cells to differentiate osteogenic cells and molecular factors that modulate cell behavior [11,12]. Cells isolated from the periosteum provide several advantages, including a multipotential capacity, easy expansion in culture, and a phenotypically stable osteogenic potential, even in elderly individuals [13–16]. In addition, periosteum-derived cells (PDCs) from different donor sites and different species have shown wide viability in their osteogenic potential [17–19]. Thus, the periosteum may provide a major source of skeletal progenitor cells for bone development and growth.

The co-culture of stem cells with other mature cells is being increasingly used to drive stem cell differentiation toward needed lineages [20–23]. Furthermore, cell sheet engineering is being studied for regenerative uses, such as for myocardial tissue, cornea, and artificial skin bone graft materials [24–26]. In theory, using a PDCs-impregnated cell sheet to surround the BMSCs-impregnated 3D scaffold might create a periosteum-bone biomimetic bone graft substitute and co-culturing environment for PDCs and BMSCs for skeletal tissue engineering strategy. The PDCs-impregnated cell sheet could be used as a cellular and morphologically relevant periosteum-like tissue. The BMSCs-impregnated tricalcium phosphate (TCP) strut could provide a biomimetic bony structure. The aims of the current study were to examine the hypothesis that using this newly developed tissue-engineered bone graft could accelerate bone formation and thus enhance spinal fusion success.

Materials and Methods

Male New Zealand White rabbits weighing 3.5 to 4 kg were used in the study. Approval was obtained from the Institutional Animal Care and Use Committee at the authors' institute before the study.

Preparation of BMSCs

The methods used for isolation and cultivation of the New Zealand White rabbit BMSCs are as described in our previous study [27]. About 10 mL of bone marrow was aspirated from the iliac crest under sterile conditions into a syringe containing 6000 units of heparin. The marrow sample was washed with Dulbecco's phosphate-buffered saline (PBS) and disaggregated by passing the sample gently through a 21-gauge catheter and syringe to produce a single-cell suspension. Cells were recovered after centrifugation at 600*g* for 10 minutes. Up to 2×10^8 nucleated cells in 5 mL Dulbecco's PBS were loaded onto a 25-mL Percoll cushion (Pharmacia Biotech, Piscataway, NJ) with a density of 1.073 g/mL in a 50-mL conical tube. Cells were separated by centrifugation at 1,100*g* for 40 minutes at 20°C. Nucleated cells were collected from the interface, diluted with two volumes of Dulbecco's PBS, and centrifuged at 900*g*. The cells were then resuspended, counted, and plated at 2×10^5 cells/cm^2 in T-75 flasks (Falcon). The cells were maintained in Dulbecco's modified Eagle's medium (Gibco BRL; Life Technologies, Gaithersburg, MD) containing 10% fetal bovine serum (HyClone, South Logan, UT) and antibiotics (100 units/mL penicillin mixed with 100 μg/mL streptomycin; Gibco) at 37°C in a humidified atmosphere of 5% CO_2 and 95% air. After 4 days of primary culturing, nonadherent cells were removed by changing the medium; medium was changed every 3 days thereafter. The BMSCs, which grew as symmetrical colonies, were subcultured for 10 to 14 days with 0.05% trypsin and for 5 minutes with 0.53 mM ethylene-diamine-tetra-acetic acid, rinsed from the substrate with serum-containing medium, collected by centrifugation at 800*g* for 5 minutes, and seeded into fresh flasks at 5,000 to 6,000 cells/cm^2. Cultures were incubated in a humidified atmosphere of 5% CO_2 and 95% air until cell confluence was achieved. Three-passaged cells were used. Cell number and viability were assessed with a hemocytometer.

Preparation of PDCs

The methods used for isolation and cultivation of the rabbit PDCs are as described in previous study [23]. PDCs were obtained by stripping the periosteum of the distal femoral and proximal tibial metaphyses of New Zealand White rabbits. The periosteum was digested in a0.25% trypsin solution and 0.1% ethylene-diamine-tetra-acetic acid for 30 minutes at 37°C and shaken in 1 mg/mL of type 1 collagenase digestive solution for 90 minutes at 37°C. After washing and centrifugation, the pellets were resuspended in

high-glucose Dulbecco's modified Eagle's medium supplemented with 10% fetal bovine serum and 1% penicillin-streptomycin (Biological Industries, Kibbutz BeitHaemek, Israel). PDCs were finely plated in a T25 culture flask (Corning Inc., Acton, MA, USA). Nonadherent cells were removed by changing the fresh medium after 5 days of culture. The culture medium was replenished every 3 days. The fibroblast cells were removed by partial trypsinization. First, the media was vacuumed off. Then, the cells were washed with PBS, the 0.05% trypsin solution was added, and the cells were incubated for 5 minutes at 37˚C, 5% CO_2. This caused the fibroblasts to change shape and lift off the plate. The trypsin and fibroblasts were vacuumed off and the cells were washed with PBS once more. Both procedures were performed at least four times until the cells were devoid of fibroblasts, leaving only PDCs in culture.

Preparation of artificial periosteal cell sheet

To prepare polymer solutions for electrospinning, medical grade polycaprolactone (PCL) with an average molecular weight (Mw) of 80,000 Da (Sigma-Aldrich, St. Louis, USA) was dissolved in hexafluoroisopropanol (Sigma) at 15% (w/v). The PCL solution was placed in a glass syringe and driven by a syringe pump with a constant volume flow rate. The polymer solution flowed through a Teflon tube (Alltech, inner diameter: 0.76 mm) to a stainless steel spinneret (Hamilton, inner diameter: 0.41 mm), and then positive high-voltage was applied to the tip of the syringe spinneret through a wire. During this process, a strong electrical field was created between the polymer solution within the spinneret and the collector. After the electrical field had beaten a critical value to overcome the surface tension of the polymer solution, an electrically charged jet was ejected from the conical tip. The polymer fibers were then collected through a rotation cylinder at a constant rotated speed. The conditions of the above procedures were as follows: the applied electron voltage for electrospinning was 18 kV, the flow rate of PCL solution was 1 mL/h, the distance between the spinneret and the collector was 20 cm, the whole system was at room temperature, and the collector was a 200-rpm rotation cylinder. The fiber membrane was collated on the surface of a roll of paper. The operation was continued for 8 hours in order to obtain smooth and random fibrous PCL membranes. After the electrospinning process, the PCL membranes were dried in a vacuum at room temperature overnight to remove residual solvent for further characterization and applications.

Preparation of PDCs-loaded periosteal sheet and cellular observation

The PDCs were trypsinized and resuspended in the medium and were pipetted and seeded uniformly onto the periosteal sheet scaffold (2.5×10^4 cells/cm^2). The cells/sheet implants were cultured overnight before implantation. The samples were fixed using 3% glutaraldehyde and 2% paraformaldehyde in 0.1 M cacadylate buffer (pH7.4) for 2 hours at 4˚C, washed with 0.1 M cacadylate buffer, fixed using 1% osmium teteroxide in cacadylate buffer for 1 hour at 4˚C, and washed with cacadylate buffer. For the scanning electron microscopy (SEM) analysis, the specimens were dehydrated through a graded series of ethanol solutions, beginning with a 50% solution and progressing through 70%, 95%, and 100% solutions. The specimens were dried in a HCP-2 critical-point dryer (Hitachi, Tokyo, Japan) and were sputter-coated using an IB.3 ion coater (EiKo, Japan). Finally, the samples were visualized using a field emission SEM (Hitachi S-5000, Tokyo, Japan) to evaluate cell adherence and growth. PDCs successfully seeded onto the artificial periosteal sheet were confirmed by SEM analysis (Fig. 1).

Preparation of BMSCs-loaded TCP and cellular observation

A porous TCP scaffold (60% by weight hydroxyapatite and 40% by weight β-TCP) (Wiltrom Co., Hsinchu,

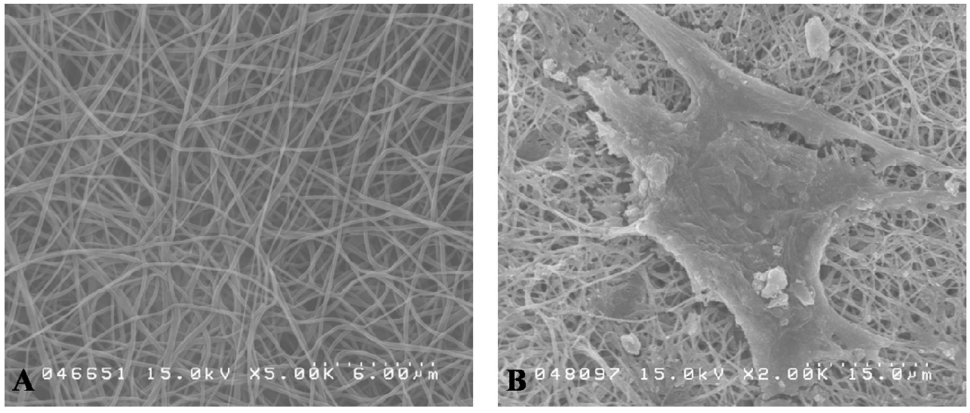

Fig. 1. Scanning electron micrograph of the electrospun mesh artificial cell sheet. (Left) The cell sheet showing a three-dimensional structure with smooth polycaprolactone fibers. (Right) The periosteum-derived cells are seen successfully seeded onto the cell sheet scaffold.

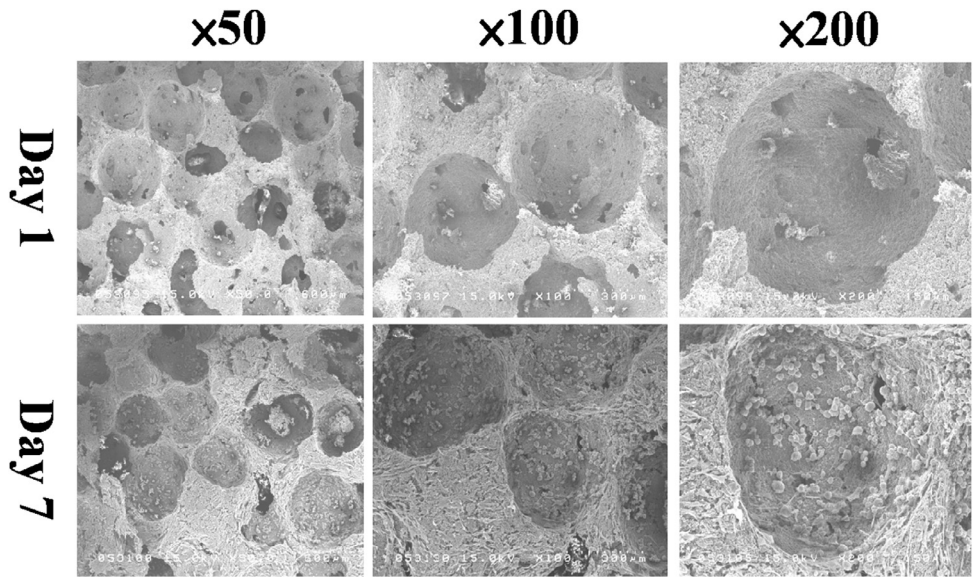

Fig. 2. Scanning electron micrograph of the porous TCP scaffold. The images of Day 7 showing bone marrow derived mesenchymal stem cells successfully attached and proliferated within the TCP scaffold when compared with images of Day 1. TCP, tricalcium phosphate.

Taiwan) with a pore size of 300 to 600 μm and porosity of 70% was used as the carrier for BMSCs delivery. The TCP was sterilized with 70% alcohol and prewetted with fresh medium overnight before use. The BMSCs were trypsinized and resuspended into the medium and were pipetted and seeded uniformly onto the TCP scaffold (4×10^6 cells/cm^3). The cells/scaffold was cultured overnight before implantation. Evaluation of cells seeded onto the TCP scaffold was determined by SEM analysis (Fig. 2).

In vivo animal experiment

Eighteen male New Zealand White rabbits were divided into three groups according to the material (Fig. 3) implanted into the bilateral L4-5 intertransverse space and survived for 12 weeks for final analysis of fusion success: (group 1) TCP wrapped with a PDCs-free periosteal sheet (n=6); (group 2) BMSCs-loaded TCP wrapped with a PDCs-free periosteal sheet (n=6); (group 3) BMSCs-loaded TCP wrapped with a PDCs-loaded periosteal sheet (n=6). In order to determine whether the bone formation was initiated during the early stage or not, two additional rabbits were operated in each experimental group and were sacrificed at 4 weeks and 8 weeks. The L4–L5 fusion segments were retrieved for histologic examinations to evaluate new bone formation after 4 and 8 weeks' implantation. Under anesthesia with an intramuscular injection of Zoletil (10 mg/kgw) (Virbac Laboratories, Carros, France), all studied animals underwent intertransverse fusion at the L4–L5 level with different bone graft materials. Under aseptic conditions, the bilateral L4 and L5 transverse processes were exposed and were decorticated by electric burr. The bone

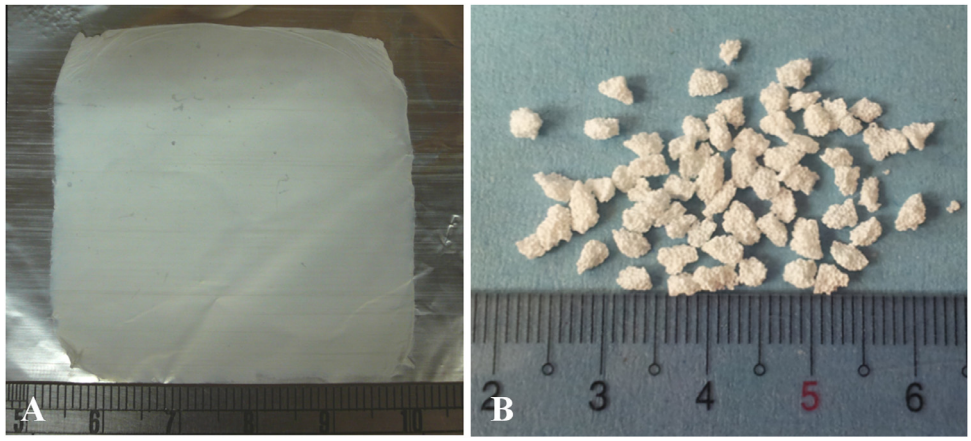

Fig. 3. Entire pictures of the electrospun mesh artificial cell sheet and tricalcium phosphate. (Left) The artificial cell sheet is a white and thin membrane collated on the surface of paper. (Right) The porous tricalcium phosphate granule scaffold before cell sheet wrapping.

graft material (3 mL) was then placed on each side between the transverse processes. The fascia and skin were closed layer-by-layer with absorbable sutures. After operation, all animals received 200 mg cefamezine per day for 3 days. The animals were allowed unlimited activity without brace application.

Radiographic analysis

All of the rabbits underwent 2-mm thin-cut computed tomography (CT) scanning of the lumbosacral spine at 12 weeks. The radiographic analysis of the fusion status was performed by two independent reviewers who were blinded to the test and animals. New bone formation in the fusion area and in any unintended area such as the spinal canal was examined by axial, coronal, and sagittal planes 3D reconstructed images. Fusion results were defined as union and nonunion. Radiographic nonunion was determined when empty spaces were found between the TCP granules. Successful radiographic fusion was defined as continuous calcified materials formation between the TCP granules and an uninterrupted bridge between the intertransverse processes on coronal and sagittal reconstructed CT scan images [28]. The right and left intertransverse fusion areas were collected separately for statistical analysis.

Manual palpation of spine fusion

After 12 weeks of survival, the rabbits were sacrificed and L3–L6 was excised en bloc from the animals after taking CT scans. The analysis was performed by two independent reviewers who were blinded to the study groups. The whole specimens were dissected and the residual muscles were gently removed. After that, the L4–L5 fusion segment was loaded in cantilever bending and manipulated gently to avoid producing gross trauma, but enough to evaluate gross intervertebral motion. Only those fusion segments identified as not having gross motion were considered to be solid union.

Mechanical testing

After manual palpation, the L4–L5 segments were stabilized along the longitudinal axis in epoxy blocks that were cylindrically shaped (3.5 cm radii and 2-cm thick). Because the size of the rabbit vertebral body is relatively small, we found that it was not easy to provide a good fixation for further biomechanical test if the embedded parts only include inferior L4 and superior L5 vertebral body. So, the embedded structures included L3, L3–L4 disc, L5–L6 disc, and L6 for providing enough fixing strength of the L4–L5 fusion segment for further biomechanical testing. The length of the L4–L5 nonembedded portion of each specimen was identical (Fig. 4, Left). The specimens were then secured on a mechanical strength machine (Gotech Testing Machines, Inc., Taichung, Taiwan) for rotational torque and toughness assessments (Fig. 4, Right). The maximum torque values were obtained from the torque-rotation angle curve. The results were presented as means ± standard deviation.

Histology evaluation

The en bloc spine specimens were fixed in 10% neutral buffered formaldehyde, decalcified, dehydrated through alcohol gradients, cleared, and embedded in paraffin blocks. Tissue blocks of the intertransverse fusion areas were sectioned and stained with hematoxylin and eosin (H&E) and

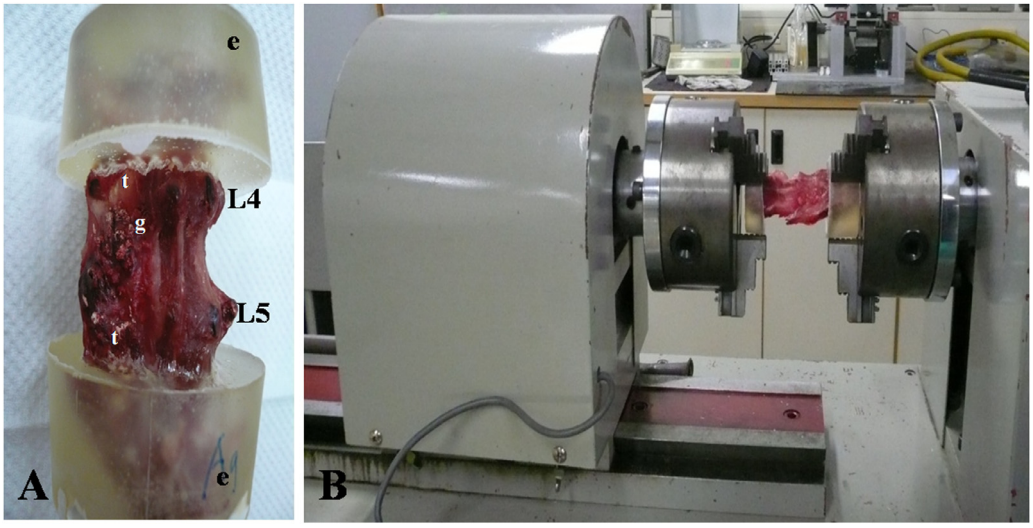

Fig. 4. Entire pictures of the embedded L4–L5 epoxy block and biomechanical testing. (Left) The spine specimen was embedded and only kept the L4–L5 portion for further biomechanical testing. Besides, the TCP granule was not absorbed although new bony mass formed between the L4–L5 transverse process in the specimen. (Right) The specimen was then secured on a mechanical strength machine for rotational torque and toughness assessments. TCP, tricalcium phosphate; e, epoxy; g, TCP granule; L4, L4 spinous process; L5, L5 spinous process; t, transverse process.

Masson's trichrome methods, and visualized using standard light microscopy. Immunohistochemical analysis for collagen type 1 and osteocalcin was also performed. The new bone formation and any inflammatory response to the grafts were subsequently assessed.

Statistical analysis

Statistical analyses were performed using the Statistical Package for the Social Sciences for Windows (SPSS, version 12.0; IBM, Armonk, NY, USA). Differences in radiographic and manual palpation results among groups were analyzed by Fisher's exact test. Differences in mechanical testing results among groups were analyzed via Kruskal-Wallis test. When a significant difference was found, a Mann-Whitney *U* test between groups was then performed. The level of statistical significance was set at .05.

Results

All animals were tolerant to the surgical procedures. Table 1 lists the results of fusion rates and manual palpation in each group. Table 2 lists the data of average maximal torques at failure among groups.

Radiographic analysis

Each group had 12 radiographic fusion areas, because the right and left intertransverse fusion areas were collected separately. Using the definition of successful radiographic fusion described above, fusion success was zero in group 1, 3 in group 2, and 9 in group 3. Radiographic findings for all rabbits in group 1 showed empty spaces without calcified material formation between the TCP granules. However, continuous ossified material formation between the TCP granules was found on the CT scan images of rabbits in group 3 with successful fusion (Fig. 5). In addition, all experimental animals showed no new bone formation in any unintended areas. Statistical analysis showed that group 3 had significantly better fusion success than groups 1 and 2 ($p < .001$).

Manual palpation

The TCP granules were not absorbed completely by gross inspection in all specimens from three experimental groups. In all six specimens of group 1, the L4–L5 segment was mobile without solid fusion between the transverse processes. However, one solid fusion existed in group 2, and five solid fusions were found in group 3. Among them, one rabbit in group 3 had unilateral union on radiographs that was revealed as solid fusion by manual palpation. Group 3 had a higher successful solid fusion rate than group 1 or 2. Statistical analysis by Fisher's exact test showed statistically significant differences among groups (p=.005).

Table 1
Results of the radiographic fusion area and manual palpation in each group

	Fusions	
	No./Total radiographs	No./Total manual palpations
Group 1	0/12 (0%)	0/6 (0%)
Group 2	3/12 (25%)	1/6 (16.7%)
Group 3	9/12 (75%)	5/6 (83.3%)

Table 2
Results of the average maximal torques at failure among groups

	Group 1	Group 2	Group 3
1	970.73	697.11	1187.94
2	763.44	557.77	931.85
3	672.35	502.27	852.82
4	576.53	695.51	688.32
5	650.28	682.73	747.49
Average	727±136	627±91	882±195

Mechanical testing

The average maximal torques at failure was 727±136 N mm, 627±91 N mm, and 882±195 N mm for groups 1, 2, and 3, respectively. The statistical difference among groups was not significant using the Kruskal-Wallis test (p=.085). Of note, the maximal torque was significantly higher in group 3 than in group 2, using the Mann-Whitney *U* test (p=.028).

Histology evaluation

After 12 weeks of survival, the TCP granules were not completely degraded in specimens from all experimental groups. There was no evidence of inflammatory reaction to the artificial cell sheets and TCP materials, because no lymphocytic cells were detected. New bone formation was indicated by H&E staining and mature bone was confirmed by Masson's trichrome staining (Fig. 6). In the specimens from group 1, there was no bone formation and only dense connective tissue between TCP granules at 4 and 8 weeks. Some bone formation within the TCP granules was found at 12 weeks. The specimens from group 2 exhibited bone formation within the TCP granules at 8 and 12 weeks, but without continuous bony connection. Meanwhile, the specimens from group 3 displayed bone formation within the TCP granules at 4 weeks and had a greater bone formation with continuous bony bridge between TCP granules at 8 and 12 weeks. Blood vessels and cells within the fusion mass were also detected by H&E staining. The results of histological evaluation verified that new bone regeneration was greater in the sample from group 3 than from groups 1 and 2 at all three different survival durations. Besides, immunohistochemical staining analysis of the L4–L5 specimens following 4 and 8 weeks' bone graft implantation from different treatment groups displayed that group 3 had greater new bone, collagen type 1, and osteocalcin formation within and between the TCP granules (Fig. 7).

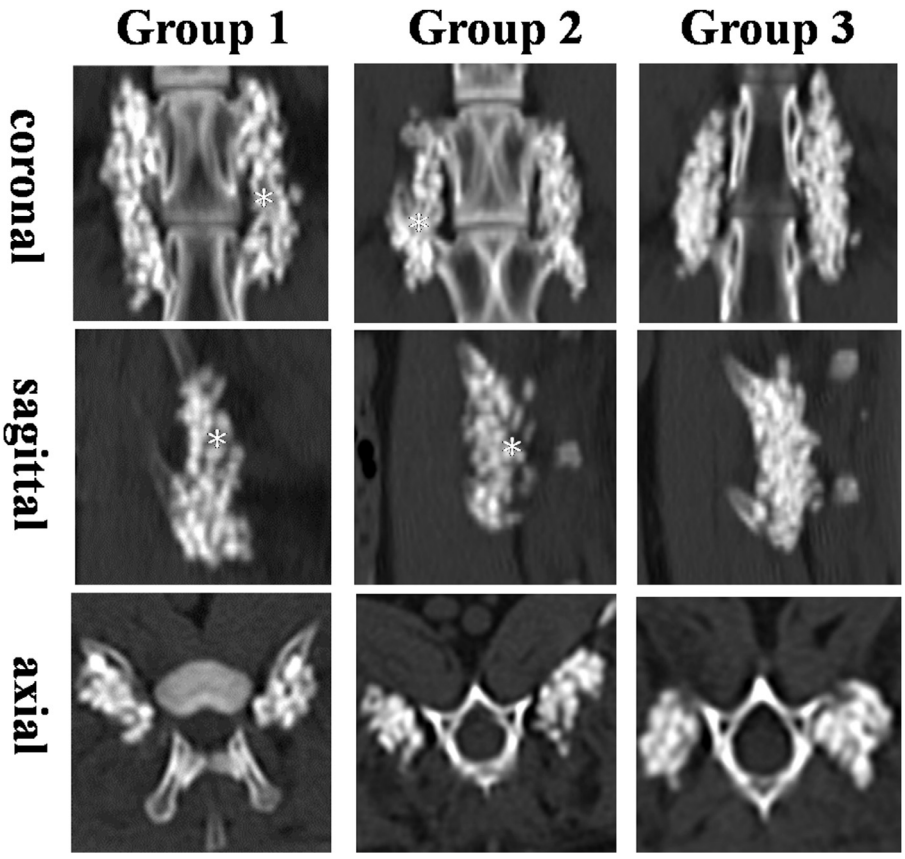

Fig. 5. Three-dimensional reconstructive CT scanning at 12 weeks showed continuous ossification between the TCP granules on the coronal, sagittal, and axial CT images in group 3. * indicates the empty spaces without continuously ossification between the TCP granules in groups 1 and 2. CT, computed tomography; TCP, tricalcium phosphate.

The findings indicated that the synergetic effect of BMSCs and PDCs in bone formation was initiated during the early stage after bone graft implantation.

Discussion

Development of a periosteum-bone biomimetic bone graft substitute could be a promising approach to cell-based bone tissue engineering for bone regenerative therapy. The results of the current study showed that the use of BMSCs-loaded TCP wrapped with a PDCs-loaded artificial cell sheet facilitated new bone formation for spine fusion, as assessed by in vivo tissue morphology studies. Using a PDCs-impregnated cell sheet to surround the BMSCs-impregnated TCP scaffold not only created a periosteum-bone biomimetic bone graft but also provided a possible co-culturing environment for further interaction between PDCs and BMSCs.

Co-culture of different cells provides a relatively new approach to overcoming the deficits of single-cell culture in vivo [20]. Co-culture of MSCs with other mature cells to drive stem cell differentiation toward the needed lineages has been increasingly used [22]. Interactions between the two types of cells occurred and cell behaviors changed by either direct or indirect cell contacts. The reason why indirect co-culture of cells can enhance osteogenic expression is unclear. The microenvironment and extracellular matrix (ECM) formed by cells may play a crucial role in osteogenic differentiation because these cells were not directly contacted. ECM is produced by cells and plays a key role in cell migration, attachment, and cell development. It provides an appropriate microenvironment to support cell adhesion and direct cell behaviors, such as proliferation and differentiation [29–31]. Although the current study did not analyze the detailed factors of ECM produced by PDCs and BMSCs, the current results presumed that cell-derived ECM either from PDCs or BMSCs may guide both cells to osteoblastic differentiation.

Although this investigation showed that periosteum-bone biomimetic bone graft substitute could be useful for bone regenerative therapy in rabbit spine intertransverse fusion, cells themselves and interactions between cells still play important roles in this new intervention. BMSCs-loaded TCP wrapped with a PDCs-loaded cell sheet had significantly higher osteogenic capacity than TCP wrapped with a PDCs-free cell sheet. This indicated that PDCs play a critically important role in BMSC differentiation. Without PDCs, an artificial cell sheet alone cannot enhance the osteogenic capacity of BMSCs. However, a combination of different kinds of cells may stimulate or suppress the

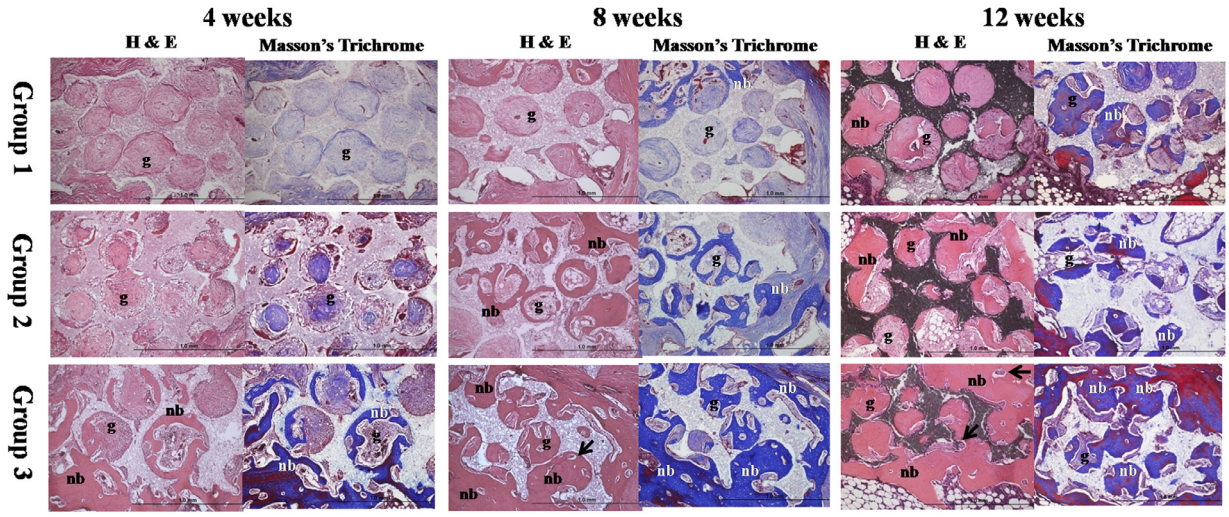

Fig. 6. Histological sections of the fusion areas underwent H&E staining and Masson's trichrome stainingin different treatment groups harvested following 4, 8, and 12 weeks. The specimens from group 3 displayed greater mature bone formation within and between the TCP granules especially at 8 and 12 postoperative weeks. Specimens from group 1 had only some bone formation within the TCP granules at 8 and 12 weeks. Although some bone formation was present in specimens from group 2 at 8 and 12 weeks, most was found within the TCP granules without continuous connection. Blood vessels and cells within the specimens from group 3 were also detected (black arrows). H&E, hematoxylin and eosin; TCP, tricalcium phosphate; g, TCP granule; nb, new bone.

proliferation and expansion of each cell. In the current study, the total dsDNA content of cultured cells was not examined because we were interested purely in the end effect of combined PDCs and BMSCs. Besides, it is difficult to differentiate the individual contribution of either PDCs or BMSCs because the total gene expression was a product of both types of cells. Further investigation is necessary to elucidate the interaction between PDCs and BMSCs in terms of cell proliferation and potential inflammatory reactions.

The periosteum consists of multipotent mesodermal cells that are capable of differentiating into osteogenic cells, and

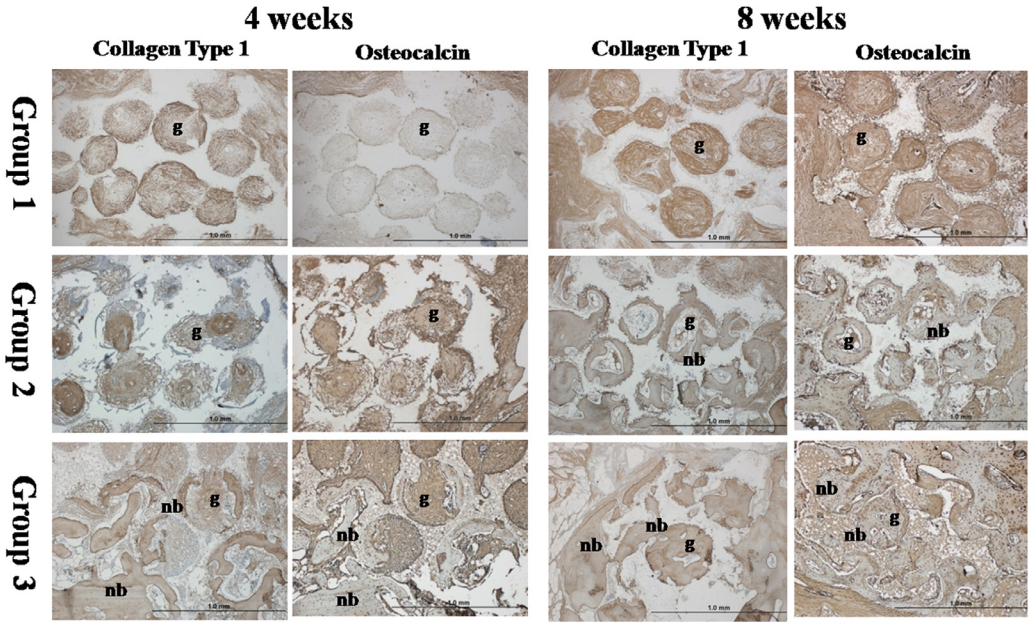

Fig. 7. Histological sections of the fusion areas underwent immunohistochemical (IHC) staining for collagen type 1 and osteocalcin in different treatment groups harvested following 4 and 8 weeks. The specimens from group 3 displayed continuous new bone and osteocalcin formation within and between the TCP granules at both 4 and 8 postoperative weeks. The findings indicated that the synergetic effect of BMSCs and PDCs in bone formation was initiated during the early stage after bone graft implantation. BMSCs, bone marrow derived mesenchymal stem cells; PDCs, periosteum-derived cells; g, TCP granule; nb, new bone.

has been shown to accelerate bone and tendon repair by potentially providing a source of progenitor cells and molecular factors that modulate cell behavior [26]. From the structural perspective, the inner cambium layer of the periosteum directly lines the outer surface of the bone and consists mostly of progenitor cells that constantly build and repair bone. Periosteal progenitor cells are critical for endochondral bone formation in cortical healing. They may contribute to healing through cell proliferation, differentiation and/or the release of paracrine signals, resulting in recruitment and activation ofosteogenic cells [32]. These findings and our current results have highlighted the potential of using progenitor cells derived from periosteum as a new source for regenerative medicine.

For bony tissue engineering, an ideal biodegradable scaffold is important in providing a 3D framework to act as a temporary matrix for cellular adhesion, proliferation, differentiation, and new bone formation at the implanted site. Furthermore, the scaffold should have the ability to deliver and retain cells at the site requiring bone production without inhibiting bone formation or eliciting an inflammatory reaction. In the present study, TCP was used as a cell carrier because it offers a 3D frame work and is biocompatible, and has been used clinically. The cells were successfully seeded onto a TCP scaffold and further cell growth was proved by the SEM analysis. The histologic results also revealed no inflammatory reaction in the host. The BMSCs were successfully transferred to the host using this 3D carrier system. However, TCP showed low biodegradability and displayed an unfavorable resorption property, which interfered with the detection of new bone formation by plain radiographs only [28]. In this study, CT scan was used as the primary tool to evaluate bone fusion by interpreting the presence and calcification of new bone formation between the TCP granules.

The concept of cell-sheet technology for tissue engineering and regeneration was first used by Okano et al. The smart surface of the cell sheet allows the implantation of cells by hydrophilic/hydrophobic transition of the substrate, which avoids using chemicals and does not affect cell viability [33]. Several cell-sheet technology application methods using collagen gel scaffold, small intestinal submucosa matrix, or thrombin-fibrinogen membrane without scaffold have been reported recently [26,32,34]. The current study used an electrospun mesh artificial cell sheet. Using SEM analysis, the PDCs were proved to be adherent and grew on the artificial cell sheet. The electrospun mesh cell sheet provided a 3D construct and an efficient way of delivering PDCs for migration, adherence and proliferation. In terms of mechanical strength, the electrospun artificial cell sheet is as weak as periosteum. We used the artificial cell sheet only for delivering cells and for wrapping the TCP constructand did not use it for mechanical support.

Although mechanical testing has become a very accepted means of spine fusion assessment, manual palpation has been accepted as an alternative method for spine fusion evaluation though it is relatively subjective and will induce bias by observers. By manual palpation, the spine specimens are palpated for intervertebral motion analogous to manual testing at surgical exploration in humans. Although more precise and quantitative pull-apart testing or multidirectional flexibility testing has been established for certain models, the accuracy of such testing has been remarkably similar to simpler manual testing techniques [35]. If the fusion was not solid, we can easily find that there was still movement between the spinous process and the fusion area by manual palpation. In the current study, we used both biomechanical testing and manually palpation to confirm the fusion success.

Despite the encouraging results in our study, some limitations of this study should be addressed. First, the results of current study cannot tell the behavior change and the growth rate of both transplanted PDCs and BMSCs within the cell sheet bone graft system. Whether the transplanted cells themselves underwent full differentiation into osteogenic cells or just induce the osteogenic differentiation of surrounding host cells was unknown. Further investigation is necessary to elucidate the interactions between the transplanted cells and the host cells in terms of cell proliferation and differentiation. Second, the current study did not use the digitalized measuring equipment to evaluate the new bone formation. The areas of new bone formations can be objectively counted numerically by numbers of pixels and measuring the percentages of areas of new bone formation per histological slide. The numerical data could make easy to analyze the results and clear the thesis of current study. Third, the current study did not have a study group with autogenous bone graft to compare to the other groups. As the principle of our Institutional Animal Care and Use Committee is to decrease the necessary number of the experimental animals as possible for statistical analysis and based on our previous results of using autogenous bone graft for rabbit posterolateral spine fusion [36,37], we only compared the fusion success for designed bone graft substitutes and not to do the autogenous iliac bone graft group for comparison for studies after 2009 [27,28].

In conclusion, this study describes the feasibility of using a PDCs-impregnated cell sheet to surround the BMSCs-impregnated TCP scaffold for creating a periosteum-bone biomimetic bone graft substitute to enhance bone regeneration and posterolateral fusion success. This novel tissue engineering approach not only created a periosteum-bone biomimetic bone graft but also might provide a co-culturing environment for these two cells. These findings implicate a relatively new approach to improve bone regeneration and spine fusion.

Acknowledgments

This work was supported by grants (CMRPG290453) received from Chang Gung Memorial Hospital, Taiwan.

References

[1] Banwart JC, Asher MA, Hassanein RS. Iliac crest bone graft harvest donor site morbidity. A statistical evaluation. Spine 1995;20:1055–60.

[2] Gamradt SC, Lieberman JR. Genetic modification of stem cells to enhance bone repair. Ann Biomed Eng 2004;32:136–47.

[3] Younger EM, Chapman MW. Morbidity at bone graft donor sites. J Orthop Trauma 1989;3:192–5.

[4] Hutmacher DW. Scaffolds in tissue engineering bone and cartilage. Biomaterials 2000;21:2529–43.

[5] Bruder SP, Jaiswal N, Ricalton NS, Mosca JD, Kraus KH, Kadiyala S. Mesenchymal stem cells in osteobiology and applied bone regeneration. Clin Orthop 1998;355:247–56.

[6] Marcacci M, Kon E, Moukhachev V, Lavroukov A, Kutepov S, Quarto R, et al. Stem cells associated with macroporous bioceramics for long bone repair: 6- to 7-year outcome of a pilot clinical study. Tissue Eng 2007;13:947–55.

[7] Pittenger MF, Mackay AM, Beck SC, Jaiswal RK, Douglas R, Mosca JD, et al. Multilineage potential of adult human mesenchymal stem cells. Science 1999;284:143–7.

[8] Solchaga LA, Johnstone B, Yoo JU, Goldberg VM, Caplan AI. High variability in rabbit bone marrow-derived mesenchymal cell preparations. Cell Transplant 1999;8:511–9.

[9] Bruder SP, Jaiswal N, Haynesworth SE. Growth kinetics, self-renewal, and the osteogenic potential of purified human mesenchymal stem cells during extensive subcultivation and following cryopreservation. J Cell Biochem 1997;64:278–94.

[10] Mueller SM, Glowacki J. Age-related decline in the osteogenic potential of human bone marrow cells cultured in three-dimensional collagen sponges. J Cell Biochem 2001;82:583–90.

[11] Chang H, Knothe Tate ML. Concise review: the periosteum: tapping into a reservoir of clinically useful progenitor cells. Stem Cells Transl Med 2012;1:480–91.

[12] Colnot C, Zhang X, Knothe Tate ML. Current insights on the regenerative potential of the periosteum: molecular, cellular, and endogenous engineering approaches. J Orthop Res 2012;30:1869–78.

[13] Chen D, Shen H, Shao J, Jiang Y, Lu J, He Y, et al. Superior mineralization and neovascularization capacity of adult human metaphyseal periosteum-derived cells for skeletal tissue engineering applications. Int J Mol Med 2011;27:707–13.

[14] Choi YS, Noh SE, Lim SM, Lee CW, Kim CS, Im MW, et al. Multipotency and growth characteristic of periosteum-derived progenitor cells for chondrogenic, osteogenic, and adipogenic differentiation. Biotechnol Lett 2008;30:593–601.

[15] Koshihara Y, Hirano M, Kawamura M, Oda H, Higaki S. Mineralization ability of cultured human osteoblast-like periosteal cells does not decline with aging. J Gerontol 1991;46:201–6.

[16] Park BW, Hah YS, Kim DR, Kim JR, Byun JH. Osteogenic phenotypes and mineralization of cultured human periosteal-derived cells. Arch Oral Biol 2007;52:983–9.

[17] Eyckmans J, Luyten FP. Species specificity of ectopic bone formation using periosteum-derived mesenchymal progenitor cells. Tissue Eng 2006;12:2203–13.

[18] McDuffee LA, Anderson GI. In vitro comparison of equine cancellous bone graft donor sites and tibial periosteum as sources of viable osteoprogenitors. Vet Surg 2003;32:455–63.

[19] Roberts SJ, van Gastel N, Carmeliet G, Luyten FP. Uncovering the periosteum for skeletal regeneration: the stem cell that lies beneath. Bone 2015;70:10–8.

[20] Qing C, Wei-ding C, Wei-min F. Co-culture of chondrocytes and bone marrow mesenchymal stem cells in vitro enhances the expression of cartilaginous extracellular matrix components. Braz J Med Biol Res 2011;44:303–10.

[21] Rangappa S, Entwistle JW, Wechsler AS, Kresh JY. Cardiomyocyte-mediated contact programs human mesenchymal stem cells to express cardiogenic phenotype. J Thorac Cardiovasc Surg 2003;126:124–32.

[22] Sui Y, Clarke T, Khillan JS. Limb bud progenitor cells induce differentiation of pluripotent embryonic stem cells into chondrogenic lineage. Differentiation 2003;71:578–85.

[23] Chang CH, Chen CH, Su CY, Liu HT, Yu CM. Rotator cuff repair with periosteum for enhancing tendon-bone healing: a biomechanical and histological study in rabbits. Knee Surg Sports Traumatol Arthrosc 2009;17:1447–53.

[25] Masuda S, Shimizu T, Yamato M, Okano T. Cell sheet engineering for heart tissue repair. Adv Drug Deliv Rev 2008;60:277–85.

[26] Nishida K. Tissue engineering of the cornea. Cornea 2003;22(Suppl 7):S28–34.

[27] Syed-Picard FN, Shah GA, Costello BJ, Sfeir C. Regeneration of periosteum by human bone marrow stromal cells sheets. J Oral Maxillofac Surg 2014;72:1078–83.

[27] Fu TS, Ueng SWN, Tsai TT, Chen LH, Lin SS, Chen WJ. Effect of hyperbaric oxygen on mesenchymal stem cells for lumbar fusion in vivo. BMC Musculoskelet Disord 2010;11:52.

[28] Fu TS, Chang YH, Wong CB, Wang IC, Tsai TT, Lai PL, et al. Mesenchymal stem cells expressing baculovirus-engineered BMP-2 and VEGF enhance posterolateral spine fusion in a rabbit model. Spine J 2015;15:2036–44.

[29] Badylak SF, Freytes DO, Gilbert TW. Extracellular matrix as a biological scaffold material: structure and function. Acta Biomater 2009;5:1–13.

[30] Kleinman HK, Luckenbill-Edds L, Cannon FW, Sephel GC. Use of extracellular matrix components for cell culture. Anal Biochem 1987;166:1–13.

[31] Reilly GC, Engler AJ. Intrinsic extracellular matrix properties regulate stem cell differentiation. J Biomech 2010;43:55–62.

[32] Hoffman MD, Xie C, Zhang X, Benoit DS. The effect of mesenchymal stem cells delivered via hydrogel-basedtissue engineered periosteum on bone allograft healing. Biomaterial 2013;34:8887–98.

[33] Okano T, Yamada N, Sakai H, Sakurai Y. A novel recovery system for cultured cells using plasma-treated polystyrene dishes grafted with poly(N-isopropylacrylamide). J Biomed Mater Res 1993;27:1243–51.

[34] Chang CH, Chen CH, Liu HW, Whu SW, Chen SH, Tsai CL, et al. Bioengineered periosteal progenitor cell sheets to enhance tendon-bone healing in a bone tunnel. Biomed J 2012;35:473–80.

[35] Drespe IH, Polzhofer GK, Turner AS, Grauer JN. Animal models for spinal fusion. Spine J 2005;6:209–16.

[36] Chen WJ, Lai PL, Chang CH, Lee MS, Chen CH, Tai CL. The effect of hyperbaric oxygen therapy on spinal fusion: using the model of posterolateral intertransverse fusion in rabbits. J Trauma 2002;52:333–8.

[37] Fu TS, Chen WJ, Chen LH, Lin SS, Liu SJ, Ueng SW. Enhancement of posterolateral lumbar spine fusion using low-dose rhBMP-2 and cultured marrow stromal cells. J Orthop Res 2009;27:380–4.